

# 9-Mercaptodethiobiotin Is Generated as a Ligand to the $[2\text{Fe}-2\text{S}]^+$ Cluster during the Reaction Catalyzed by Biotin Synthase from *Escherichia coli*

Corey J. Fugate,<sup>†</sup> Troy A. Stich,<sup>‡</sup> Esther G. Kim,<sup>‡</sup> William K. Myers,<sup>‡</sup> R. David Britt,<sup>\*‡</sup> and Joseph T. Jarrett<sup>\*‡</sup>

<sup>†</sup>Department of Chemistry, University of Hawai'i at Manoa, Honolulu, Hawaii 96822, United States

<sup>‡</sup>Department of Chemistry, University of California—Davis, Davis, California 95616, United States

**S** Supporting Information

**ABSTRACT:** Biotin synthase catalyzes formation of the thiophane ring through stepwise substitution of a sulfur atom for hydrogen atoms at the C9 and C6 positions of dethiobiotin. Biotin synthase is a radical *S*-adenosylmethionine (SAM) enzyme that reductively cleaves *S*-adenosylmethionine, generating 5'-deoxyadenosyl radicals that initially abstract a hydrogen atom from the C9 position of dethiobiotin. We have proposed that the resulting dethiobiotinyl radical is quenched by the  $\mu$ -sulfide of the nearby  $[2\text{Fe}-2\text{S}]^{2+}$  cluster, resulting in coupled formation of 9-mercaptodethiobiotin and a reduced  $[2\text{Fe}-2\text{S}]^+$  cluster. This reduced FeS cluster is observed by electron paramagnetic resonance spectroscopy as a mixture of two orthorhombic spin systems. In the present work, we use isotopically labeled 9-mercaptodethiobiotin and enzyme to probe the ligand environment of the  $[2\text{Fe}-2\text{S}]^+$  cluster in this reaction intermediate. Hyperfine sublevel correlation spectroscopy (HYSCORE) spectra exhibit strong cross-peaks demonstrating strong isotropic coupling of the nuclear spin with the paramagnetic center. The hyperfine coupling constants are consistent with a structural model for the reaction intermediate in which 9-mercaptodethiobiotin is covalently coordinated to the remnant  $[2\text{Fe}-2\text{S}]^+$  cluster.

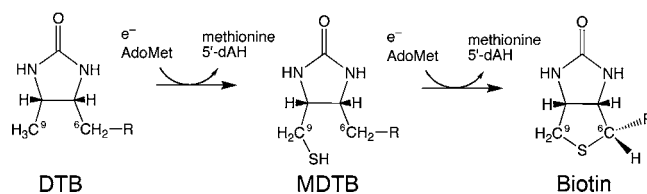
The formation of new C–S bonds at unactivated carbon centers represents a particularly challenging reaction for an enzyme catalyst.<sup>1–5</sup> The unactivated carbon center must become oxidized and have one or more hydrogen atoms removed, a process that might typically involve molecular oxygen and a metal cofactor. However, sulfur tends to be preferentially oxidized instead of carbon, and for this reason metal–oxygen chemistry is not generally used to activate the carbon center during the formation of C–S bonds.<sup>6</sup>

Recently, a number of enzymes in the radical SAM superfamily have been identified that catalyze the formation of C–S bonds.<sup>1,3,7</sup> Radical SAM enzymes catalyze the one-electron reduction of the sulfonium of *S*-adenosylmethionine (SAM or AdoMet), generating methionine and a transient 5'-deoxyadenosyl radical (5'-dA•).<sup>8</sup> This radical is a strong oxidant that can remove a hydrogen atom from a variety of organic substrates, generating high-energy substrate radicals

that can undergo further reactions to generate a variety of products.<sup>8</sup> Two radical SAM enzymes catalyze the addition of sulfur at unactivated aliphatic carbon atoms: lipoyl synthase catalyzes the addition of two thiol groups at the C6 methylene and C8 methyl positions of octanoyl-E2 protein or H protein,<sup>10,11</sup> and biotin synthase (BS) catalyzes formation of a thioether between the C6 methylene and C9 methyl positions of dethiobiotin (DTB).<sup>12–14</sup>

With BS, we have demonstrated that the addition of a single sulfur atom proceeds in a stepwise manner.<sup>15</sup> During the first half turnover, reductive cleavage of AdoMet produces a transient 5'-dA• radical that abstracts a hydrogen atom from the C9 position of DTB (Scheme 1).<sup>16</sup> The resulting 9-

## Scheme 1. Stepwise Reaction Catalyzed by Biotin Synthase



dethiobiotinyl radical adds a sulfur atom to generate 9-mercaptodethiobiotin (MDTB) as a stable chemical intermediate that is not released from the enzyme.<sup>15</sup> Exchange of methionine and 5'-deoxyadenosine (5'-dAH) for a second equivalent of AdoMet, followed by generation of a second 5'-dA• radical, facilitates abstraction of a hydrogen atom from the C6 position and thiophane ring closure. Isotopic labeling studies suggest that, during the first turnover, the sulfur atom incorporated into the thiophane ring likely derives from one of the sulfides of a  $[2\text{Fe}-2\text{S}]^{2+}$  cluster tightly bound within the core of the as-purified enzyme.<sup>17</sup>

Formation of a carbon–sulfur bond between a dethiobiotinyl carbon radical and sulfide requires concurrent one-electron oxidation. If the sulfide is donated by a  $[2\text{Fe}-2\text{S}]^{2+}$  cluster, the excess electron is likely shed into the cluster, resulting in reduction to a paramagnetic  $\text{Fe}^{\text{II}}\text{Fe}^{\text{III}}$  spin system. Using electron paramagnetic resonance (EPR) spectroscopy, we have observed formation and decay of a paramagnetic species

Received: February 21, 2012

Published: May 18, 2012

exhibiting an overlap of two orthorhombic spectra.<sup>18,19</sup> The total spin concentration approximately correlates with the concentration of MDTB at various time intervals, consistent with the simultaneous formation of these two reaction intermediates.<sup>19</sup>

Although these experimental results are consistent with an intermediate state in which the enzyme contains both tightly bound MDTB and some form of a  $[2\text{Fe}-2\text{S}]^+$  cluster, there is considerable uncertainty regarding the precise structure and electronic state of this transient intermediate. In the structure of *E. coli* BS with DTB and AdoMet bound,<sup>20</sup> the C9 position of DTB is located  $\sim 4.6$  Å (center-to-center) from the nearest  $\mu$ -sulfide of the  $[2\text{Fe}-2\text{S}]^{2+}$  cluster, while a typical carbon–sulfur bond length is  $\sim 1.7$  Å. We have previously proposed that the enzyme intermediate incorporates MDTB as a bridging thiolate ligand to the  $[2\text{Fe}-\text{S}(\text{RS})]^+$  cluster (Figure 1B),<sup>15</sup> which would

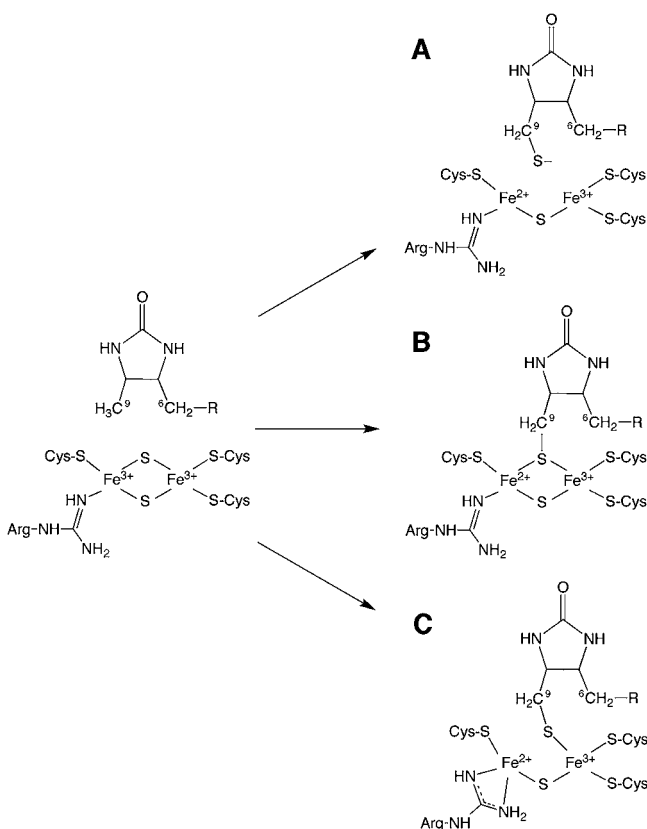


**Figure 1.** Three alternative structures for the BS intermediate state. (A) Formation of MDTB as a distal free thiolate that is ion-paired with the remnant  $[2\text{Fe}-1\text{S}]^{3+}$  cluster. (B) Formation of MDTB as a symmetric bridging ligand in the  $[2\text{Fe}-\text{S}(\text{RS})]^+$  cluster. (C) Formation of MDTB as a ligand to one Fe within the remnant  $[2\text{Fe}-1\text{S}]^{3+}$  cluster.

require a significant conformational change, as the C9 carbon atom would need to move by  $\sim 2.9$  Å to form the C–S bond. Alternatively, the sulfide could be released from the cluster and migrate to the C9 position of DTB, generating MDTB that is proximal to but not covalently attached to the remnant  $[2\text{Fe}-1\text{S}]^{3+}$  cluster (Figure 1A). Other scenarios can be envisioned in which MDTB remains as a ligand to only one Fe within the cluster (Figure 1C).

To further probe the structure of the BS reaction intermediate, we produced two isotopically labeled samples

that incorporate nuclear spins that would be in the vicinity of the reduced FeS cluster on the enzyme. Starting from (3-methyl- $^{13}\text{C}$ )-L-alanine and pimelic acid, we used BioW from *B. sphaericus* and BioF, BioA, and BioD from *E. coli*, along with the appropriate substrates and cofactors, to produce (9-methyl- $^{13}\text{C}$ )-DTB (>99% isotopic incorporation; see Supporting Information for a detailed protocol). NMR and LCMS analyses confirmed the structure and the level of isotopic incorporation. Starting with (guanidino- $^{15}\text{N}_2$ )-L-arginine fed to a  $\Delta\text{argH}$  *E. coli* expression strain, we expressed and purified BS in which all arginine residues are labeled in the terminal guanidino positions (>98% isotopic incorporation). The isotopic incorporation was confirmed by matrix-assisted laser-desorption-ionization mass spectrometry (MALDI MS) analysis of peptides produced from labeled BS by digestion with trypsin.

Samples of BS were trapped in an intermediate state containing MDTB and a paramagnetic FeS cluster in a manner similar to previous reports.<sup>15,19</sup> Briefly, the catalytic  $[4\text{Fe}-4\text{S}]^{2+}$  cluster in BS was reconstituted by incubation with  $\text{Fe}^{3+}$ ,  $\text{S}^{2-}$ , and dithiothreitol. The enzyme was then preincubated with DTB, and the biological reducing system consisted of flavodoxin, ferredoxin(flavodoxin):NADP<sup>+</sup> oxidoreductase, and NADPH. Finally, AdoMet (1 equiv per BS monomer) was added to initiate the reaction. After 30–60 min, samples were transferred to EPR tubes and frozen in liquid  $\text{N}_2$  for spectroscopic analysis. In parallel, samples were also quenched in acid for HPLC analysis of MDTB and biotin formation.

Hyperfine sublevel correlation spectroscopy (HYSCORE) is a two-dimensional pulse EPR technique that correlates nuclear spin-flip transition frequencies in one electron-spin manifold to those in another connected to the first by an EPR transition.<sup>21</sup> Correlations are typically observed between nuclear frequencies of the same nucleus, which, in the case of spin systems with multiple hyperfine-coupled nuclei, can greatly aid in the assignment of spectral features.

In the HYSCORE spectrum of the paramagnetic intermediate generated upon mixing natural abundance BS with AdoMet and DTB in the presence of the flavodoxin reducing system, several intense correlation ridges are observed with frequencies similar to those measured using three-pulse electron spin echo envelope modulation (ESEEM) spectroscopy (Figure 2, top).<sup>19</sup> These features in the ESEEM spectra were previously assigned as arising from nitrogen atoms in the guanidino group of Arg260, a conserved ligand to the  $[2\text{Fe}-2\text{S}]$  cluster,<sup>20</sup> based on the absence of these features in spectra collected under identical conditions for the active Arg260Met mutant enzyme.<sup>19</sup> This assignment is confirmed by the HYSCORE spectrum of the BS intermediate obtained using a wild-type enzyme isolated from a  $\Delta\text{argH}$  *E. coli* expression strain grown in media supplemented with (guanidino- $^{15}\text{N}_2$ )-L-arginine (Figure 2, bottom). Two sets of correlation ridges are present: one set centered at (0.82, 3.56 MHz) in the  $+-$  quadrant and one set centered at (1.08, 1.97 MHz) in the  $++$  quadrant that are respectively diagnostic of the presence of both strongly and weakly hyperfine-coupled  $^{15}\text{N}$  nuclei. The more strongly coupled class of  $^{15}\text{N}$  nuclei likely corresponds to the iron-ligated nitrogen atom(s) of the guanidino group of Arg260 (Figure 1). It is possible that both guanidino nitrogen atoms lie in a similar coordination environment relative to the FeS cluster, as depicted in Figure 1C, giving rise to a single set of cross peaks in the  $+-$  quadrant. The weakly coupled  $^{15}\text{N}$  nuclei could be due to the nearby Arg95 residue, which is hydrogen bonded to Arg260 in the crystal structure ( $d_{\text{Fe}-\text{N}} =$

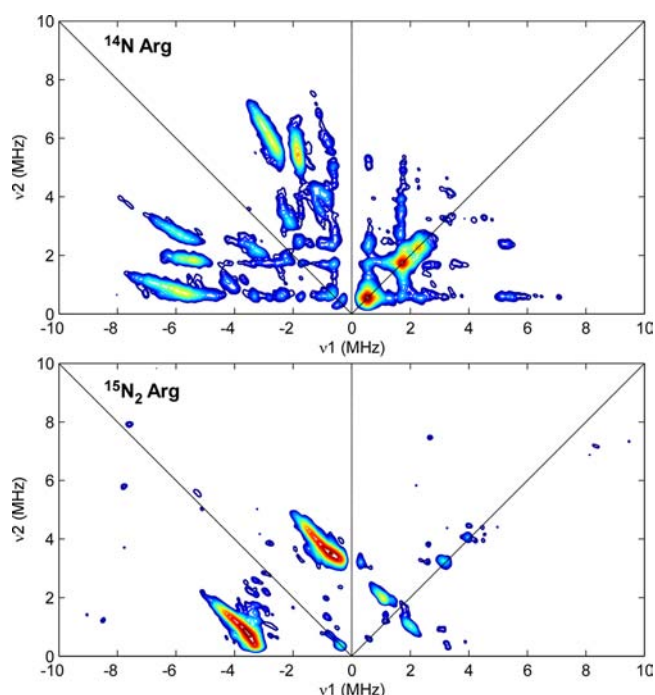


**Figure 2.** HYSORE spectra of the BS paramagnetic intermediate produced in BS purified from *E. coli* grown with natural abundance arginine (top) and (*guanidino*- $^{15}\text{N}_2$ )-L-arginine (bottom). Spectrometer settings: (top) excitation frequency = 9.363 GHz;  $\tau$  = 136 ns; (bottom) excitation frequency = 9.419 GHz;  $\tau$  = 132 ns. All other settings were identical: temperature = 10 K;  $B_0$  = 347.5 mT;  $t_{\pi/2} = t_{\pi} = 16$  ns;  $t_1 = t_2 = 100$  ns;  $\Delta t = 20$  ns.

5–7 Å).<sup>20</sup> This assignment would perhaps explain the prior observation of residual  $^{14}\text{N}$  peaks in the three-pulse ESEEM spectrum of the Arg260Met mutant enzyme.<sup>19</sup> However, based on the crystal structure of the oxidized form of wild-type BS, the guanidino nitrogens of Arg95 are too distant to account for the observed hyperfine anisotropy (see Supporting Information) without invoking a substantial reorganization of the active site upon formation of the paramagnetic intermediate. Alternatively, the weakly coupled  $^{15}\text{N}$  nucleus could correspond to the uncoordinated nitrogen of the guanidino group as depicted in Figure 1B. This assignment is supported by the small  $A_{\text{iso}} = 0.57$  MHz determined for these features (see Figure S10 in the Supporting Information).

The HYSORE spectrum of the paramagnetic intermediate generated using natural abundance BS and (9-methyl- $^{13}\text{C}$ )-DTB (Figure 3B) possesses correlation ridges centered at (2.9, 4.7 MHz) and (4.7, 2.9 MHz) that extend for nearly 1 MHz and have no counterpart in the corresponding natural abundance spectrum (Figure 3A). The position and field-dependence of these features are well-simulated using an axial  $^{13}\text{C}$  hyperfine interaction (HFI) of [1.2, 1.2, 5.7] MHz and electron  $g$ -values = [1.995, 1.941, 1.849], determined previously for the major spectral component (64–74%) of the EPR spectrum (see Figure S9).<sup>19</sup> Although the EPR spectra (Figure S12) contain two components that can be simulated using two possible combinations of four distinct  $g$ -tensors,<sup>19</sup> the HFI is not strongly dependent on the particular set of  $g$ -values used in the simulation (see Table S1 and Figure S10). The nature of the structural or electronic difference between major and minor components in the EPR spectrum is presently not understood. Field-dependent HYSORE spectra show no evidence of two

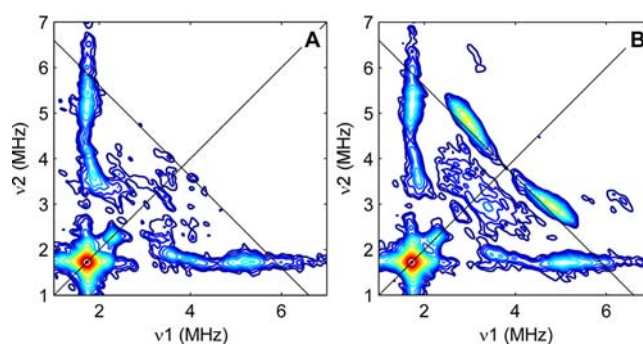


**Figure 3.** HYSORE spectra of the BS paramagnetic intermediate prepared with (A) natural abundance DTB and (B) (9-methyl- $^{13}\text{C}$ )-DTB. Spectrometer settings: excitation frequency = 9.75 GHz; temperature = 10 K;  $B_0$  = 355 mT;  $t_{\pi/2} = t_{\pi} = 16$  ns;  $\tau$  = 132 ns;  $t_1 = t_2 = 100$  ns;  $\Delta t = 20$  ns.

distinct sets of  $^{13}\text{C}$  correlation ridges that would suggest the presence of two species with different hyperfine couplings for C9 of MDTB. This finding could indicate that (i) the  $^{13}\text{C}$  hyperfine interaction is identical for both forms of the  $[2\text{Fe}-2\text{S}]^+$  cluster observed as major and minor components in the EPR spectra, or (ii) for one of the forms, there are no observable  $^{13}\text{C}$  couplings (i.e., MDTB is not bound or the coupling is too inhomogeneous to observe).

Multinuclear coherences lead to the weak features centered at (3.0, 6.3) and (6.3, 3.0) in the (9-methyl- $^{13}\text{C}$ )-DTB/BS spectrum. The 6.3 MHz frequency is a combination of one of the  $^{13}\text{C}$  frequencies (4.7 MHz) with the  $^{14}\text{N}$ -associated frequency (1.7 MHz). This behavior results when nuclear transition frequencies from different nuclei but within the same electron spin manifold (e.g.,  $m_S = +1/2$ ) are correlated to a frequency in the opposite electron spin manifold (e.g.,  $m_S = -1/2$ ).<sup>22</sup> That these multinuclear coherences appear requires that both nuclei are hyperfine-coupled to the same electron spin; thus, C9 is interacting directly with the  $[2\text{Fe}-2\text{S}]^+$  cluster that is hyperfine-coupled to an arginine residue, presumably Arg260, as depicted in Figure 1B or 1C.

The strength of the  $^{13}\text{C}$  hyperfine interaction is significant as disclosed by the relatively large isotropic contribution to the hyperfine tensor ( $A_{\text{iso}} = 2.7$  MHz). For comparison, in the Radical SAM superfamily member pyruvate formate lyase-activating enzyme (PFL-AE), the methyl group of AdoMet is spatially close to but not bound to the  $[4\text{Fe}-4\text{S}]^+$  cluster ( $d_{\text{Fe-C}} = 3.5$  Å),<sup>23</sup> and ENDOR spectra exhibit an effective  $A_{\text{iso}} < 0.3$  MHz.<sup>23</sup> Alternatively, carbon atoms that are covalently bonded to heteroatoms coordinated to the Fe atoms of FeS clusters can have  $A_{\text{iso}}$  values ranging from 3 to 17 MHz (see Table 1). The anisotropic contribution to the  $^{13}\text{C}$  hyperfine interaction is also relatively large ( $T = 1.5$  MHz), corroborating the close association of C9 with the  $[2\text{Fe}-2\text{S}]^+$  cluster. The effective  $^{13}\text{C}$  isotropic hyperfine interaction reported here for (9-methyl- $^{13}\text{C}$ )-DTB/BS is most similar to that found for the  $\beta$ -C of the cysteine ligands to the  $\text{Fe}^{\text{II}}\text{Fe}^{\text{III}}$  form of ferredoxin.<sup>25</sup> This would be consistent with a structural model of the BS reaction intermediate in which MDTB is formed as a ligand to the remnants of the  $[2\text{Fe}-2\text{S}]$  cluster.

The spectroscopic data are most consistent with a mechanism in which 5'-dA• abstracts a hydrogen atom from the C9 position of dethiobiotin, and the dethiobiotinyl radical moves  $\sim 2.9$  Å to attack the  $\mu$ -sulfide of the  $[2\text{Fe}-2\text{S}]^{2+}$  cluster. Since DTB is held in place primarily through hydrogen bonds

**Table 1.**  $^{13}\text{C}$  Hyperfine Couplings in Fe Cluster Spin Systems

system	$M_{\text{ox}}$	$^{13}\text{C}$ HFI (MHz)	ref.
MMOH + DMSO <sup>a</sup>	$\text{Fe}^{\text{II}}\text{Fe}^{\text{III}}$	~1.3	26
PFL-AE + SAM <sup>b</sup>	$[\text{4Fe-4S}]^+$	[-0.6, +0.4, -0.5]	24
IspG + MEcPP <sup>c</sup>	$[\text{4Fe-4S}]^+$	C2 = [14.5, 12.0, 26.5] C3 = [1.8, 2.0, 5.1]	27
$\text{H}_{\text{ox}}\text{-CO}^d$	$\text{Fe}^{\text{I}}\text{Fe}^{\text{II}}$	C1 = [15.6, 16.6, 19.2] C2 = [8.5, 9.8, 3.9] C3 = [3.2, 3.7, 4.4]	28
Fd <sup>e</sup>	$[\text{2Fe-2S}]^+$	C1 = 0.76–1.2 C2 = 1.9–2.1	25
BS + $^{13}\text{C}_9\text{-DTB}$	$[\text{2Fe-2S}]^+$	[1.2, 1.2, 5.7]	this study

<sup>a</sup> $^{13}\text{C}$ -DMSO + methane monooxygenase hydroxylase from *Methyl-ococcus capsulatus* (Bath). <sup>b</sup>(Methyl- $^{13}\text{C}$ )-S-adenosylmethionine + pyruvate formate-lyase activating enzyme from *E. coli*. <sup>c</sup>Reaction intermediate of (2,3- $^{13}\text{C}$ )-2-C-methylerythritol-cyclo-2,4-diphosphate with IspG from *E. coli*. <sup>d</sup> $^{13}\text{C}$ -inhibited form of  $[\text{FeFe}]$  hydrogenase from *Desulfovibrio desulfuricans*. <sup>e</sup> $^{13}\text{C}$ -enriched ferredoxin from *Anabaena*.

between the DTB imidazolidinone, Asn151, Asn153, and Asn222,<sup>20,29</sup> this attack could be accomplished through a simple hinge motion around these hydrogen bonds. The resulting MDTB intermediate then remains as a ligand to the remnant FeS cluster, likely resulting in a significant conformational rearrangement of the active site. Additional structural information regarding the precise positioning of MDTB relative to the FeS cluster and AdoMet is needed to provide a complete mechanistic description of biotin thiophane ring formation.

## ■ ASSOCIATED CONTENT

### 📄 Supporting Information

Experimental procedures for production, purification, and characterization of (9-methyl- $^{13}\text{C}$ )-DTB and (guanidino- $^{15}\text{N}_2$ )-arginine biotin synthase, procedures for generation of the paramagnetic enzyme intermediate, CW EPR spectra of all samples, and additional magnetic field-dependent HYS-CORE spectra are included in the Supporting Information. This material is available free of charge via the Internet at <http://pubs.acs.org>.

## ■ AUTHOR INFORMATION

### Corresponding Author

rdbritt@ucdavis.edu; jtj@hawaii.edu

### Notes

The authors declare no competing financial interest.

## ■ ACKNOWLEDGMENTS

This research has been supported by grants from the NSF (MCB 09-23829 to J.T.J.) and the NIH (GM73789 to R.D.B.). EPR data were collected at the CalEPR facility at UC Davis funded by the NIH (S10-RR021075) and the University of California.

## ■ REFERENCES

- (1) Booker, S. J.; Cicchillo, R. M.; Grove, T. L. *Curr. Opin. Chem. Biol.* **2007**, *11*, 543.
- (2) Marquet, A.; Florentin, D.; Ploux, O.; Tse Sum Bui, B. *J. Phys. Org. Chem.* **1998**, *11*, 529.
- (3) Fugate, C. J.; Jarrett, J. T. *Biochim. Biophys. Acta* **2012**, in press.

(4) Fontecave, M.; Ollagnier-de-Choudens, S.; Mulliez, E. *Chem. Rev.* **2003**, *103*, 2149.

(5) Marquet, A. *Curr. Opin. Chem. Biol.* **2001**, *5*, 541.

(6) The non-heme iron enzyme, isopenicillin-N-synthase, is a rare example of a metal-oxygen system that can form a C–S bond. Roach, P. L.; Clifton, I. J.; Hensgens, C. M.; Shibata, N.; Schofield, C. J.; Hajdu, J.; Baldwin, J. E. *Nature* **1997**, *387*, 827.

(7) Atta, M.; Arragain, S.; Fontecave, M.; Mulliez, E.; Hunt, J. F.; Luff, J. D.; Forouhar, F. *Biochim. Biophys. Acta* **2012**, in press.

(8) Frey, P. A.; Booker, S. J. *Adv. Protein Chem.* **2001**, *58*, 1.

(9) Frey, P. A.; Hegeman, A. D.; Ruzicka, F. J. *Crit. Rev. Biochem. Mol. Biol.* **2008**, *43*, 63.

(10) Cicchillo, R. M.; Booker, S. J. *J. Am. Chem. Soc.* **2005**, *127*, 2860.

(11) Douglas, P.; Kriek, M.; Bryant, P.; Roach, P. L. *Angew. Chem., Int. Ed.* **2006**, *45*, 5197.

(12) Mejean, A.; Bui, B. T.; Florentin, D.; Ploux, O.; Izumi, Y.; Marquet, A. *Biochem. Biophys. Res. Commun.* **1995**, *217*, 1231.

(13) Sanyal, I.; Cohen, G.; Flint, D. H. *Biochemistry* **1994**, *33*, 3625.

(14) Ugulava, N. B.; Sacanell, C. J.; Jarrett, J. T. *Biochemistry* **2001**, *40*, 8352.

(15) Taylor, A. M.; Farrar, C. E.; Jarrett, J. T. *Biochemistry* **2008**, *47*, 9309.

(16) Escalletes, F.; Florentin, D.; Tse Sum Bui, B.; Lesage, D.; Marquet, A. *J. Am. Chem. Soc.* **1999**, *121*, 3571.

(17) Farrar, C. E.; Siu, K. K.; Howell, P. L.; Jarrett, J. T. *Biochemistry* **2010**, *49*, 9985.

(18) Jameson, G. N.; Cospers, M. M.; Hernandez, H. L.; Johnson, M. K.; Huynh, B. H. *Biochemistry* **2004**, *43*, 2022.

(19) Taylor, A. M.; Stoll, S.; Britt, R. D.; Jarrett, J. T. *Biochemistry* **2011**, *50*, 7953.

(20) Berkovitch, F.; Nicolet, Y.; Wan, J. T.; Jarrett, J. T.; Drennan, C. L. *Science* **2004**, *303*, 76.

(21) Höfer, P.; Grupp, A.; Nebenführ, H.; Mehring, M. *Chem. Phys. Lett.* **1986**, *132*, 279.

(22) Stoll, S.; Calle, C.; Mitrikas, G.; Schweiger, A. *J. Magn. Reson.* **2005**, *177*, 93.

(23) Vey, J. L.; Yang, J.; Li, M.; Broderick, W. E.; Broderick, J. B.; Drennan, C. L. *Proc. Natl. Acad. Sci. U.S.A.* **2008**, *105*, 16137.

(24) Walsby, C. J.; Hong, W.; Broderick, W. E.; Cheek, J.; Ortillo, D.; Broderick, J. B.; Hoffman, B. M. *J. Am. Chem. Soc.* **2002**, *124*, 3143.

(25) Houseman, A. L. P.; Oh, B. H.; Kennedy, M. C.; Fan, C.; Werst, M. M.; Beinert, H.; Markley, J. L.; Hoffman, B. M. *Biochemistry* **1992**, *31*, 2073.

(26) DeRose, V. J.; Liu, K. E.; Lippard, S. J.; Hoffman, B. M. *J. Am. Chem. Soc.* **1996**, *118*, 121.

(27) Wang, W.; Wang, K.; Li, J.; Nellutla, S.; Smirnova, T. I.; Oldfield, E. *J. Am. Chem. Soc.* **2011**, *133*, 8400.

(28) Silakov, A.; Wenk, B.; Reijerse, E.; Albracht, S. P. J.; Lubitz, W. *J. Biol. Inorg. Chem.* **2009**, *14*, 301.

(29) Farrar, C. E.; Jarrett, J. T. *Biochemistry* **2009**, *48*, 2448.